Intrinsic point defects in crystalline silicon: Tight-binding molecular dynamics studies of self-diffusion, interstitial-vacancy recombination, and formation volumes

Meijie Tang
Lawrence Livermore National Laboratory, P.O. Box 808, L-268, Livermore, California 94550

L. Colombo
Istituto Nazionale per la Fisica della Materia and Dipartimento di Fisica Università di Milano, via Celoria 16, I-20133 Milano, Italy

Jing Zhu and T. Diaz de la Rubia
Lawrence Livermore National Laboratory, P.O. Box 808, L-268, Livermore, California 94550

(Received 7 August 1996)

Tight-binding molecular dynamics simulations are performed to study self-diffusion, interstitial-vacancy recombination, and formation volumes of point defects in crystalline silicon. The results show that (i) self-diffusion is dominated by vacancies (V) at low temperature and by interstitials (I) at high temperature; (ii) interstitial-vacancy recombination at room temperature leads to formation of a metastable I-V complex, which has an annihilation energy barrier of 1.1 eV; (iii) interstitial and vacancy relaxation volumes in silicon are approximately equal in magnitude and opposite in sign. [S0163-1829(97)03218-9]

I. INTRODUCTION

Intrinsic point defects such as vacancies and interstitials mediate mass transport in crystalline solids. While the properties of point defects are well known in metals,[1] in silicon controversy remains regarding their diffusivities and equilibrium concentrations. In addition, ion implantation of dopants into silicon is a common step in silicon device manufacturing that introduces large supersaturations of point and extended defects.[2] Upon annealing at elevated temperatures, these defects interact with the dopants and cause transient-enhanced diffusion (TED).[3] TED results in changes in the junction depth and has the potential to degrade the performance of future generation semiconductor devices. Therefore, miniaturization of electronic devices demands a thorough understanding and accurate description of the diffusion processes of both intrinsic point defects and dopants.

Over the years, considerable experimental and theoretical work has been carried out to study the structure, energetics, and migration of point defects in silicon, as well as their role in transient-enhanced diffusion. Experiments in silicon, however, have produced conflicting evidence and have resulted in intense debate, especially on the relative contribution of vacancies and interstitials to self-diffusion and substitutional dopant diffusion.[4] On the other hand, theory has made significant progress using both first-principles calculations[5–8] and atomistic simulations based on empirical interatomic potentials.[9–12] However, controversy remains regarding some of the most fundamental properties of intrinsic point defects. A number of key parameters such as the diffusivities and thermal equilibrium concentrations of vacancies and self-interstitials, as well as their formation volumes, are far from well established. In addition, and of great importance to the description of amorphization and implant damage annealing, is the issue of interstitial-vacancy annihilation and the possible existence of a barrier to mutual recombination, as has been previously suggested but never definitely shown.[13]

These fundamental questions provide a wide opportunity for theoretical studies. Some work has been done regarding Si self-diffusion[9–11] and formation volumes[10,14] using either the Stillinger-Weber (SW) empirical potential or first-principles local density approximation (LDA) calculations. The SW potential predicts the equilibrium ground-state neutral interstitial configuration to be a $\langle 110 \rangle$ dumbbell in two possible geometrical arrangements separated in energy by 0.8 eV.[15] Although this is in good qualitative agreement with recent LDA calculations, the exact geometry and relative energy of the two defects are different in the two cases.[16] In fact, the low-energy SW configuration corresponds to a high-energy defect in the LDA and vice versa. LDA calculations have also been used extensively to study the interaction between silicon defects and dopant atoms.[5,8,17] Recently, LDA calculations have also been used to study the structure and energy of divacancies in silicon.[18]

Despite the tremendous power of the LDA method to study defect properties, the technique is limited by its extremely high computational demands. While calculations that minimize the energy of an ensemble of 64 atoms in a supercell at zero temperature can be routinely done, studies of defect diffusion with accurate statistics are difficult.

In this paper, we apply the tight-binding molecular dynamics (TBMD) simulation method to study some of the fundamental aspects of intrinsic point defects and diffusion in crystalline silicon. In a TBMD simulation, the band structure energy and the many-body forces are calculated directly by diagonalizing the one-electron Hamiltonian matrix.[19] This method is much less computationally intensive than the LDA calculations and thus allows us to study larger systems with up to 216 atoms for time scales of up to hundreds of picoseconds, which is important for the description of the diffusion process. In Sec. II, we briefly describe the TBMD model used in this paper. For the study of intrinsic point defects, it is important that a model can describe the energetics and structures of the basic defects accurately. Comparisons of

formation energies with other methods including first-principles LDA calculations and classical potentials are given. In Sec. III, we present results of calculations of the self-interstitial and vacancy diffusivities. By comparing the data to experiments and other first-principles calculations, insight has been gained in understanding silicon self-diffusion. In Sec. IV, we present the first atomistic study of interstitial-vacancy recombination and annihilation. We find that the spontaneous recombination volume of an interstitial-vacancy pair is strongly dependent on crystallographic orientation. A type of metastable defect, an interstitial-vacancy (I-V) complex, is formed by the interaction of an interstitial and a vacancy. Our calculations suggest an energy barrier of 1.1 eV for the annihilation of the complex. In Sec. V, motivated by experimental measurements of relaxation volumes of point defects produced by electron irradiation in Si at low temperature,[20] we calculate the interstitial and vacancy relaxation volumes. The calculations show that these relaxation volumes cancel each other out, which agrees well with the experimental findings. Finally, we discuss the implications of these calculations for the interpretation of current experiments in Sec. VI and conclusions in Sec. VII.

II. COMPUTATIONAL FRAMEWORK

All the main issues addressed in the present investigation concern quantum mechanical phenomena involved in the bond-formation and bond-breaking mechanisms occurring during defect formation, migration, and recombination. A quantum mechanical description of the interactions at the atomic scale is, indeed, necessary. On the other hand, to perform MD simulations of defect diffusion, we need to span a time interval and a system size which hardly can be handled by first-principles LDA-based calculations. We therefore adopted the TBMD scheme where the essential quantum mechanical features are taken into account on the basis of a simple, but reliable model. The key idea of the TBMD scheme is to derive at each step of the simulation the attractive contribution to the interatomic forces from the electronic structure of the investigated sample which, in turn, is computed by an orthogonal tight-binding (TB) model solved within the two-center approximation. The total energy functional from which to derive the net force on each atom is, then, completed by a suitable effective short-range repulsive potential. Further details of the method can be found elsewhere.[19]

In this work, we make use of the TBMD model by Kwon *et al.*[21] (KBWHS model) which represents an improved release of the TBMD model for silicon presented in a seminal paper by Goodwin *et al.*[22] (GSP model). The repulsive potential is now given in the form of an embedded-atom potential and different scaling functions for the TB hopping integrals are provided, according to the actual symmetry of the selected orbitals. Finally, the short-range character of the total energy functional has been exploited so that no arbitrary cutoff for the interactions needs to be imposed. The resulting TBMD scheme is more accurate than the GSP model. In Table I, we show the formation energies obtained from the two tight-binding models and compare them with those obtained using the SW potential[9] and *ab initio* calculations.[23] For the neutral ground state of the self-interstitial, *ab initio* calculations predict the $\langle 110 \rangle$ dumbbell structure, which agrees with the prediction of the current model. The previous GSP model predicts the tetrahedral configuration as the lowest-energy structure. Notice that although the SW potential also predicts a $\langle 110 \rangle$ type of dumbbell structure as the lowest-energy configuration,[9,15] its structure is different from the dumbbell predicted by *ab initio* and tight-binding methods. The structure predicted by the SW potential is rather extended with significant distortion of the nearest-neighbor atoms along the $\langle 110 \rangle$ dumbbell direction.[15] This is due to the fact that the SW potential always tend to lower the energy by favoring the local configuration to be tetrahedral.[24]

TABLE I. Point defect formation energies calculated by the LDA (GGA) method with energy gap (correction by Zhu *et al.* (Refs. 5 and 8); current work (KBWHS), a previous TBMD model (GSP) (Ref. 22), and SW potential by Gilmer *et al.* (Ref. 9).

Defects	LDA	KBWHS	GSP	SW
Vacancy	3.65	3.97	3.96	2.64
T interstitial	5.1	4.39	4.40	4.84
H interstitial	3.8	4.93	5.90	6.58
$\langle 110 \rangle$ dumbbell	3.7	3.80	5.04	3.65 (extended)

The results presented in this work have been obtained by means of canonical or microcanonical ensemble simulations and, mostly, by using periodic supercells with 216 atoms plus (minus) the number of interstitials (vacancies) involved. To generate atomic trajectories we adopted the velocity-Verlet algorithm, with a time step as small as 10^{-15} s. Typical simulations for annealing and relaxation are performed within tens of picoseconds. As for possible size effects, we tested convergence with system size by calculating the vacancy formation energy using a 511 atom supercell: We obtained $E_f^v = 4.10$ eV with negligible change in vacancy structure. We therefore consider our numerical estimations of formation energies accurate within 0.2 eV. The defect diffusivities have been calculated using a 64-atom supercell, but much longer simulation times up to 200 ps. A check was made for our calculations using a 215 atom supercell to ensure that size effects did not play a significant role in our diffusivity results.

III. SELF-DIFFUSION

Experimental data on Si self-diffusion show that the diffusion coefficient exhibits Arrhenius behavior over a wide range of temperatures,

$$D(T) = D_0 \exp(-E_a/k_B T), \tag{1}$$

with an activation energy E_a of 4–5 eV and a preexponential factor D_0 much larger than that for typical metals.[25] Nevertheless, the relative contribution from different mechanisms, namely, from vacancies and interstitials, is still a matter of discussion. In a recent review by Gösele *et al.*,[26] the experimental data for interstitial (I) and vacancy (V) diffusion coefficients are summarized by

$$C_I^* d_I = 914 \exp(-4.84/k_B T) \quad \mathrm{cm}^2/\mathrm{sec}, \tag{2}$$

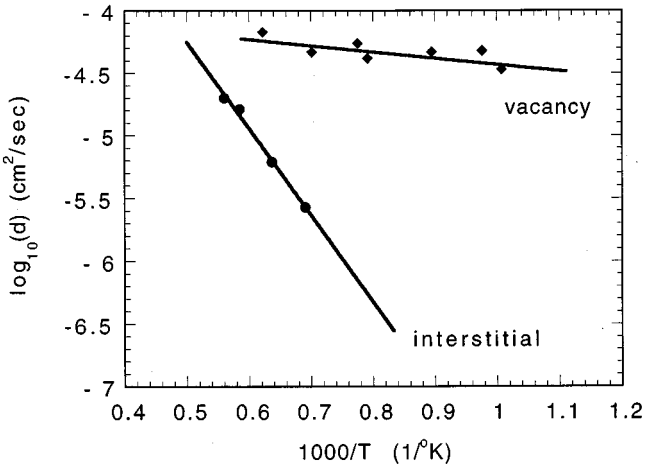

FIG. 1. Temperature-dependent diffusivities for a single vacancy (diamonds) and a self-interstitial (circles) obtained by the present TBMD calculations.

$$C_V^* d_V = 0.6\exp(-4.03/k_B T) \quad \text{cm}^2/\text{sec}, \tag{3}$$

where d_I and d_V are single defect diffusivities and C^* is equilibrium defect concentration normalized to 5×10^{22} cm^{-3}. According to Gösele *et al.*, $C_I^* d_I$ is a rather reliable and accurate quantity since two different types of experimental measurements, i.e., the U-shaped in-diffusion profiles of impurities (like Au, Pt, and Zn) and tracer diffusion experiments, give consistent results. On the other hand, the situation for the vacancy is still controversial. In addition, though $C_I^* d_I$ is well established, the individual terms of diffusivity d_I and concentration C_I^* are not known. The same holds in the vacancy case.

A theoretical determination of the self-diffusion coefficient requires three different calculations: (i) diffusivity prefactor d_0 and migration energy E_m, (ii) formation energy E_f, and (iii) formation entropy S_f. As for d_0 and E_m, they are related to the diffusivity according to the expression

$$d_{I,V} = d_{0I,V}\exp(-E_{mI,V}/k_B T), \tag{4}$$

which can be calculated during a TBMD run straightforwardly from the displacements of all atoms in the simulation cell,

$$d_{I,V} = \lim_{t\to\infty} \frac{1}{6t} \Sigma_i [\vec{r}_i(t) - \vec{r}_i(0)]^2, \tag{5}$$

which is obtained during microcanonical runs after a careful equilibration of the system. Because of the jumplike diffusion mechanism of both I and V defects[27] (see below for more details), long simulations are necessary to warrant numerical convergence. Also note that the square displacements due to thermal fluctuation without migration do not contribute to the linear slope of the total square displacements. In this work we followed vacancy and interstitial migration path for 100 ps and 200 ps, respectively. Migration energies and diffusivity prefactors are obtained by an Arrhenius interpolation of the diffusivity data, as shown in Fig. 1. The values for the migration energies are 0.1 eV and 1.37 eV for vacancies and interstitials, respectively, and the corresponding diffusivity prefactors are 1.18×10^{-4} cm^2/sec and 1.58×10^{-1} cm^2/sec. The resulting E_m value for the vacancy is likely too small, in particular in view of the experimental data of Watkins [28] which indicates a value for the neutral vacancy activation energy for migration of 0.3 eV.[29] However, it is worth noting that when combining diffusivity and formation data we obtain an overall activation energy for migration of 4.07 eV and 5.18 eV for the vacancy and interstitial, respectively. These values compare well with the experimental range 4 eV $\leqslant E_a \leqslant$ 5 eV. This seems to suggest that while the absolute numbers for E_m and E_f could probably be affected by some error, the global picture derived from these TBMD calculations of self-diffusion is qualitatively correct. It is worth noting that previous molecular dynamics investigations based on classical MD with the SW potential showed similarly that the vacancy diffusivity is larger than the interstitial diffusivity at all temperatures.[9]

The migration path for the self-interstitial has been identified by careful analysis of the computer generated trajectories. In Fig. 2, we show three snapshots taken at $T=1000$ K. The dumbbell [panel (a)] is found to move into the next tetrahedral interstitial position [panel (b)] along the $\langle 110\rangle$ direction and then move back to a dumbbell configuration [panel (c)] at the second nearest-neighbor lattice site with respect to the starting position. As for the vacancy, the migration path is obviously simpler and consists in jumps of nearest-neighbor atoms into the vacancy site.

In order to provide a complete picture of self-diffusion we still need to compute equilibrium concentrations. To this aim, an estimate of the formation entropy and energy of the individual defects is required. The latter two quantities are related to the (normalized) equilibrium concentration of the I and V defects through the relationship

$$C_{I,V}^* = \exp[-(E_f - TS_f)/k_B T]. \tag{6}$$

We have already discussed the formation energies in the previous section. In the present work we did not compute S_f by means of TBMD simulations. For vacancies, Blochl *et al.*[6] have computed the formation entropy within the thermodynamical integration theory by means of a Car-Parrinello simulation and have reported a value of $S_{fV}=9k_B$. Recently, Kajihara *et al.* have also obtained a similar number.[30] For interstitials, only a rough estimate of $S_{fI}\sim 10k_B$ is provided by Blochl *et al.*[6] We have obtained a value of the interstitial formation entropy by combining our TBMD results with the rather reliable high-temperature experimental data for $C_I^* d_I$. Since

$$C_I^* d_I = d_0 \exp(S_{fI}/k_B)\exp[-(E_f + E_m)/k_B T], \tag{7}$$

where $d_0 = 1.58\times10^{-1}$ cm^2/sec, $E_f = 3.8$ eV, and $E_m = 1.37$ eV are obtained already from our TBMD calculations, the only unknown quantity is S_{fI}. We have fitted $C_I^* d_I$ to the experimental data point at 1250 °C (Ref. 26) and obtained $S_{fI}=11.2k_B$, which is consistent with the first-principles estimate. Combining all these numbers and using Eq. (7) for both interstitials and vacancies, we can calculate the temperature dependence of the self-diffusion coefficient in silicon and compare the results to experimental data at all temperatures. An Arrhenius plot of self-diffusion including the calculation results and the experimental data as summarized

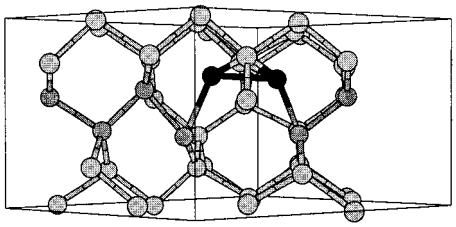

(a)

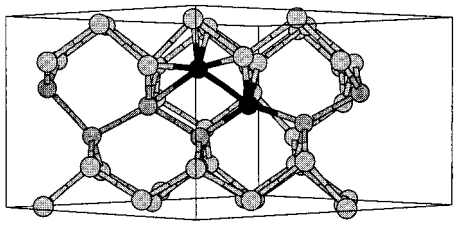

(b)

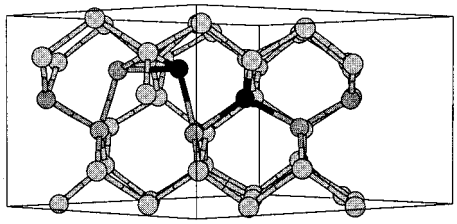

(c)

FIG. 2. Migration path for dumbbell diffusion at $T=1000$ K. The initial two dumbbell atoms are indicated by dark spheres. (a) Initial dumbbell position, (b) intermediate tetrahedral position, and (c) final dumbbell position at two nearest-neighbor distance away. The dumbbell diffusion could change direction to be along another $\langle 110 \rangle$ chain at position (b). Note that a bond is drawn if its distance is within a cutoff of 2.6 Å . Same applies to all bonds drawn in relevant figures of this paper.

by Gösele *et al.* is shown in Fig. 3. It is apparent that the TBMD results are in excellent agreement with experiments and provide a very consistent picture of self-diffusion in silicon. At low temperature, vacancies, which are the faster species in silicon, dominate self-diffusion. However, because of entropy effects (notice that the prefactor for the diffusivity is three orders of magnitude larger for interstitials than for vacancies), the interstitial dominates at high temperature. Notice also that the crossover temperature from the *I*-dominated to *V*-dominated self-diffusion regime falls at about 1080 °C. This value compares favorably with the experimental finding of 1050 °C.[4]

As mentioned above, the splitting of the $C^*_{I,V}d_{I,V}$ product into the two contributions (diffusivity and concentration) provides useful complementary information about self-

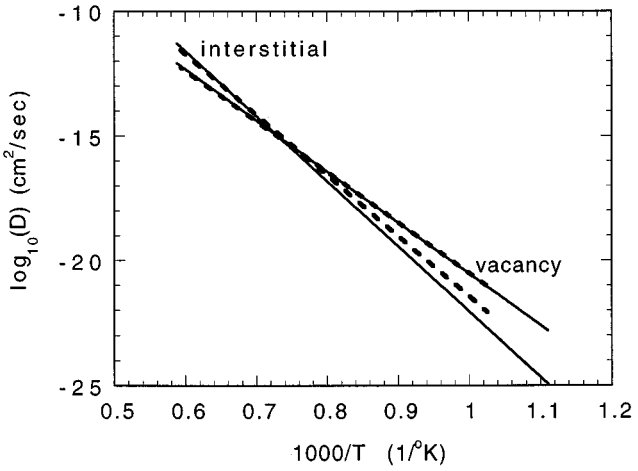

FIG. 3. Temperature-dependent self-diffusion coefficient in silicon for vacancy and self-interstitial. Solid lines, TBMD results; dashed lines, experimental data (Ref. 26).

diffusion. Using the TBMD data described above for E_f and S_f, we have determined the temperature-dependent equilibrium concentrations of interstitials and vacancies, C_I^* and C_V^*, respectively. An Arrhenius plot of these quantities (unnormalized values) is shown in Fig. 4. Also included for comparison is a plot of the equilibrium concentration of vacancies in a metal, Au, calculated using experimental data for vacancy formation energy and entropy.[1]

IV. INTERSTITIAL-VACANCY RECOMBINATION

Understanding the kinetics of interstitial-vacancy recombination is important for the development of a complete picture of implant damage annealing and dopant diffusion. Essentially, in all the continuum process simulators for dopant diffusion a plus one (+1) or similar model[31] is assumed; i.e., approximately only one interstitial per implanted ion participates in the dopant diffusion process. A fundamental assumption involved in this picture is that the interstitials and vacancies generated by ion implantation recombine and an-

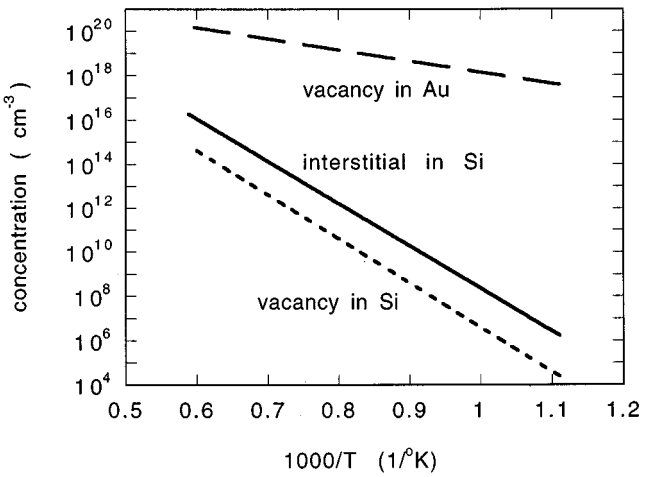

FIG. 4. Predicted interstitial (solid line) and vacancy (short dashed line) equilibrium concentrations in silicon. Also shown is the vacancy equilibrium concentration (long dashed line) in gold.

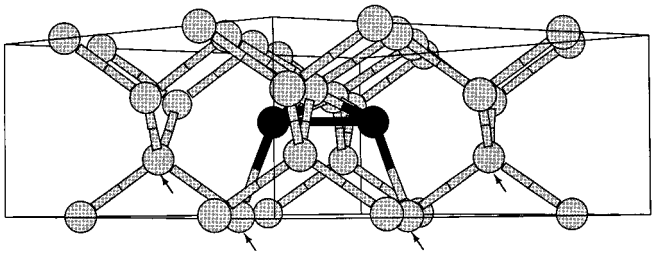

FIG. 5. Lattice sites in the vicinity of a ⟨110⟩ dumbbell. A vacancy can be created at either of these sites. Arrows indicate the vacancy sites where interstitial-vacancy recombination occurs.

nihilate very efficiently. However, the mutual recombination properties of interstitials and vacancies are not well established. In particular, in many experiments, dopants are implanted to very high concentrations and these can act as recombination centers and speed up the recombination process. In the literature, it has been found that *I-V* recombination seems to be difficult in silicon containing a low dopant concentration.[25] But whether the small recombination rate is due to an energy barrier[32] or an entropy barrier[33] is still not known. Carefully designed experiments to measure *I-V* recombination properties are missing and no theoretical calculations have been performed at the atomistic level.

Here we present results of TBMD calculations of the spontaneous recombination volume of an interstitial and a vacancy in silicon. The initial conditions of the simulation are an interstitial-vacancy pair which is separated by a particular distance along different crystallographic orientations and at room temperature. Figure 5 shows the lattice sites around a ⟨110⟩ dumbbell interstitial. A vacancy is then created by taking out one atom from one of these sites and molecular dynamics simulations are performed at 300 K to study the interaction between the dumbbell and the vacancy. In a perfect crystalline silicon lattice, one can view the structure as equivalent ⟨110⟩ chains intersecting each other at each lattice site. Once a ⟨110⟩ dumbbell is created in the crystal, anisotropy is built up along the ⟨110⟩ chains. The direction along which the ⟨110⟩ dumbbell aligns becomes a preferred direction for spontaneous *I-V* recombination. We find that spontaneous recombination occurs only for *I-V* pairs separated by first and second nearest-neighbor distances *along* the ⟨110⟩ dumbbell direction (shown by arrows in Fig. 5). In the recombination process between the *I-V* pair separated by one nearest-neighbor distance, one of the dumbbell atoms is attracted to the vacant site; at the same time, the other dumbbell atom is pulled to the regular lattice site which the dumbbell atoms shared before recombination. In the recombination process between the *I-V* pair separated by a second nearest-neighbor distance, the dumbbell migrates to the second nearest-neighbor site and annihilates with the vacancy. In Fig. 6, we show the major steps for this process. In Fig. 6(a), a vacancy is created at the second nearest-neighbor position at the beginning of the simulation; in Fig. 6(b), after 114 time steps into the simulation, the dumbbell moves to the nearest tetrahedral site towards the vacancy; in Fig. 6(c), after another 26 time steps, the tetrahedral atom moves down towards the vacancy; in Fig. 6(d), the interstitial atom moves to the location of the vacancy after anther 15 time steps. Thus, the interstitial and vacancy annihilates in about 0.155

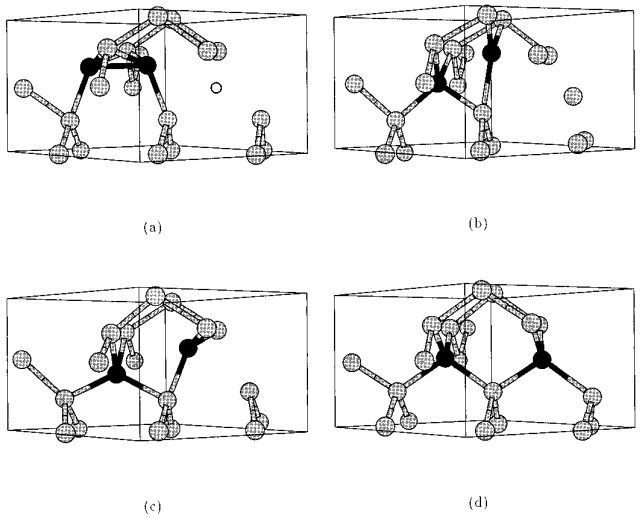

FIG. 6. Spontaneous *I-V* recombination process. (a) At $t=0$, a vacancy is created at the second nearest-neighbor position along the ⟨110⟩ dumbbell direction (shown by the open circle); (b) at $t=114$ fs, the left atom of the dumbbell moves into a regular lattice site and the right atom moves to the nearby tetrahedral site towards the vacancy; (c) at $t=140$ fs, the tetrahedral atom moves down towards the vacancy; (d) at $t=155$ fs, the interstitial atom moves to the vacancy location and the *I-V* annihilation process is complete.

psec at room temperature. This process is through the migration of the interstitial, which goes through a tetrahedral site and jumps into the second nearest-neighbor position.

We also study the interaction between *I-V* pairs separated along the ⟨110⟩ dumbbell direction by more than two nearest-neighbor spacings, up to sixth nearest-neighbor distance. In these cases, we observe that the vacancy migrates towards the ⟨110⟩ dumbbell. Upon close contact, instead of *I-V* annihilation, the interstitial and vacancy form a new defect structure at the site of the ⟨110⟩ dumbbell. Since this defect structure does not involve any excess or deficit of atoms and is formed by *I-V* interaction, we call it an *I-V complex*. Besides the ⟨110⟩ dumbbell direction, we have also studied *I-V* pairs separated along other ⟨110⟩ directions and at different distances. In all these cases, we observe similar behavior, i.e., the vacancy migrates towards the dumbbell and a *I-V* complex is formed. The reason for *I-V* complex formation instead of *I-V* annihilation is the local distortion around the ⟨110⟩ dumbbell induced by the close approach of the vacancy.

As a representative of the *I-V* complex formation process, we show in Fig. 7 the interaction between an *I-V* pair separated along the ⟨110⟩ dumbbell direction by three nearest-neighbor distances. In Fig. 7(a), the vacancy is located at the third nearest-neighbor position; in Fig. 7(b), the vacancy migrates towards the second nearest-neighbor position and the dumbbell has been pulled towards the vacancy, thus causing local distortion; in Fig. 7(c), the dumbbell is further pulled towards the vacancy and one of the dumbbell atoms (left one) almost returns to the regular lattice site; in Fig. 7(d), the *I-V* complex is formed. This process typically takes place in less than 1 psec at room temperature.

Quenching the system to zero temperature results in the low-energy *I-V* complex structure shown in Fig. 8(a). The

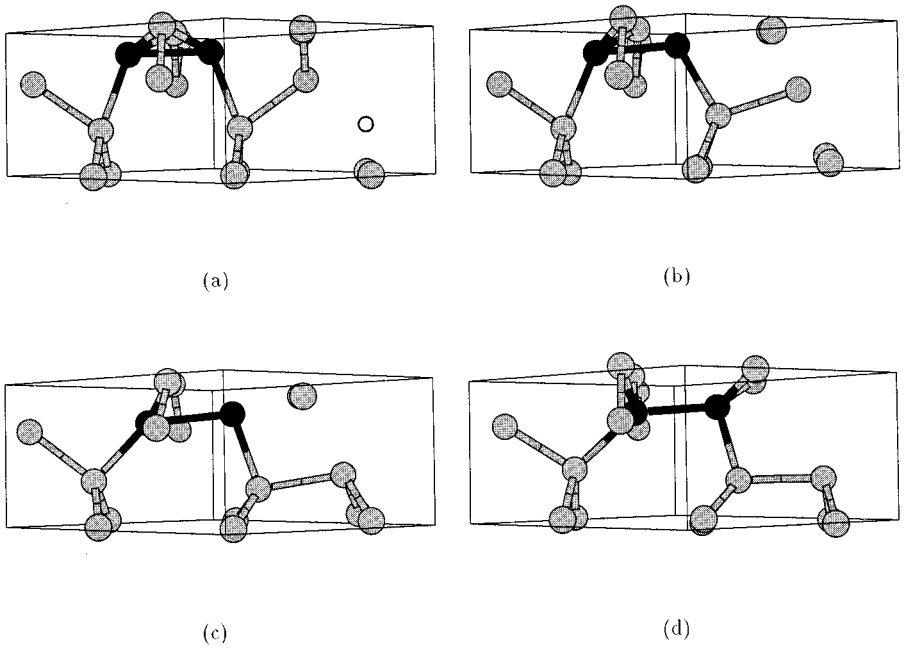

FIG. 7. *I-V* complex formation process. (a) At $t=0$, a vacancy is created at the third nearest-neighbor position along the $\langle 110 \rangle$ dumbbell direction (shown by the open circle); (b) at $t=110$ fs, the vacancy migrates towards the second nearest-neighbor position; (c) at $t=160$ fs, the vacancy further migrates towards the second nearest neighbor. Local distortion around the dumbbell occurs, where the dumbbell is pulled towards the vacancy and the left atom of the dumbbell almost returns to the regular lattice site. (d) At $t=410$ fs, vacancy migration is complete and an *I-V* complex is formed.

complex is composed of two atoms, both of which are four-fold coordinated. The two atoms are very tightly bonded to each other with a bond length of 2.28 Å (the equilibrium bond length is 2.36 Å). Also, each atom in the *I-V* complex is bonded to two regular atoms at an equal distance of 2.38 Å and to another regular atom at a longer distance of 2.46 Å . As shown below, such a configuration can be formed by switching one bond for the two *I-V* complex atoms between their first and second nearest neighbors. The formation energy of this *I-V* complex is 3.51 eV. We have also performed *ab initio* plane wave pseudopotential calculations to confirm the stability of this *I-V* complex. The results clearly show that this *I-V* complex structure is indeed a metastable state with a formation energy in the order of 3 eV.

In order to study the stability of the *I-V* complex against thermally activated processes, we perform a TBMD simulation at constant temperature of 1500 K. We find that the *I-V* complex annihilates in about 10 psec and the system recovers its defect-free crystal structure. The average lifetime τ of the *I-V* complex at different temperatures can be estimated by

$$\frac{1}{\tau} \sim \nu \exp(-E_b/k_B T), \tag{8}$$

where ν is estimated as the Debye frequency of $\sim 10^{13}$ Hz, and E_b is the energy barrier against annihilation. We first use the high-temperature molecular dynamics simulation at 1500 K to identify the annihilation path, and then perform static relaxation at zero temperature to obtain the energy barrier. The annihilation path is identified to be a bond-switching process. The major steps are shown in Fig. 8. During this process, the two long bonds in Fig. 8(a) will be broken progressively. Figure 8(b) shows the configuration after the long bonds are broken; after a saddle point configuration shown in Fig. 8(c), the two *I-V* complex atoms continue to move [Fig. 8(d)] and begin to form new bonds with their regular nearest neighbor atoms and result in the perfect diamond lattice structure shown in Fig. 8(e). In this static relaxation procedure, the two *I-V* complex atoms are moved systematically towards their final positions. At each step, the two *I-V* complex atoms are constrained to relax only in the plane perpendicular to the direction connecting their initial and final positions, while all other atoms are fully relaxed without constraint. The energy barrier thus obtained is 1.23 eV.

Since the above process requires the two *I-V* complex atoms to behave symmetrically, i.e., to break and to form bonds simultaneously, a lower energy barrier may be possible in a slightly different process, where one bond can be broken or formed before the other. To obtain the energy barrier for this process, we pick the top atom as a driving atom and move it systematically towards its final position. At each step of movement, this atom is constrained to relax in the plane perpendicular to the direction connecting its initial and final position, while all other atoms are fully relaxed. Note that in this process the second *I-V* complex atom is allowed to relax without constraint including in the direction connecting its initial and final positions. The energy barrier found in this process is 1.13 eV. Therefore, the energy barrier for the *I-V* complex to annihilate is $E_b=1.13$ eV. Using Eq. (8), we plot the estimated lifetime of the *I-V* complex at different temperatures in Fig. 9. The estimated average lifetime of the *I-V* complex at room temperature is in the order of hours, but only a few microseconds at typical annealing temperatures.

V. FORMATION VOLUMES

The formation of a vacancy or an interstitial defect in a crystal results in a volume change. First, there is a volume increase (decrease) of approximately one atomic volume on the surface for the formation of a vacancy (interstitial). This volume change is due to the replacement of the removed atom from the inside (surface) of a crystal to the surface (inside) for a vacancy (interstitial). Second, there is usually a

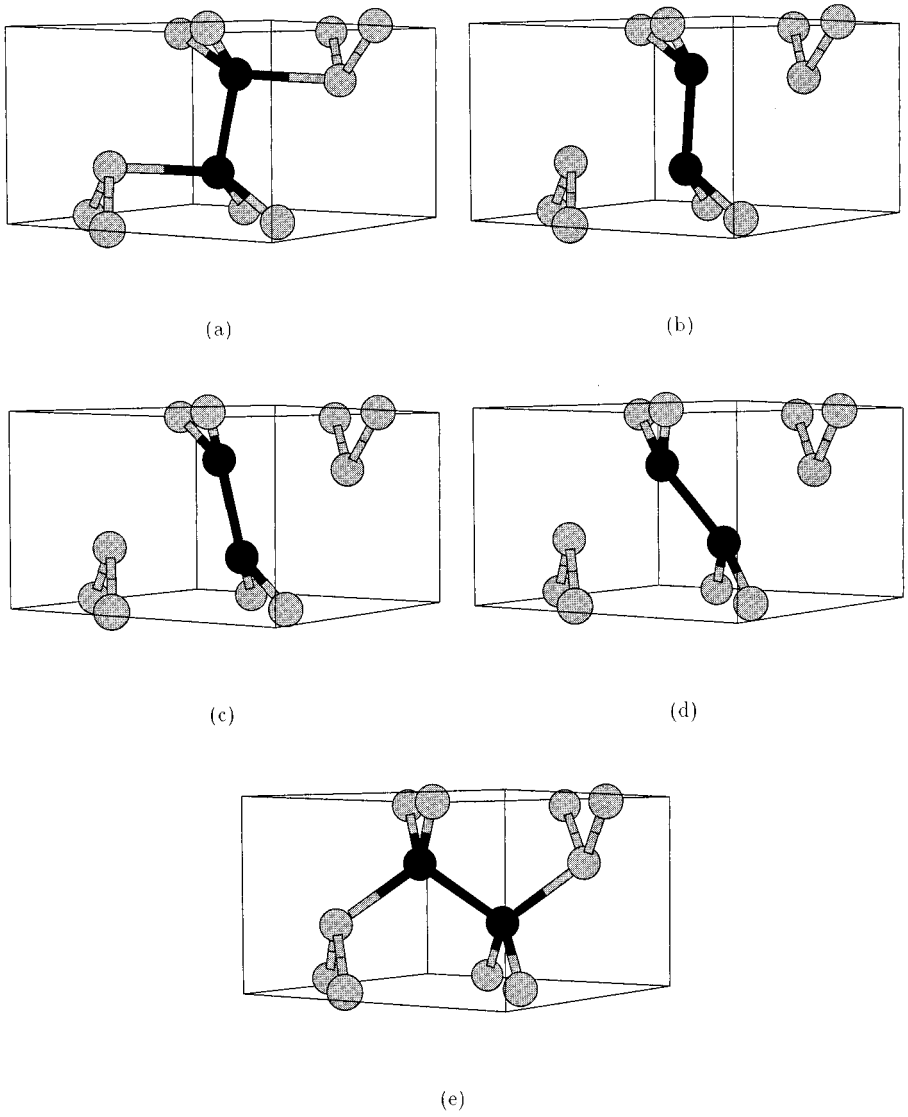

FIG. 8. *I-V* complex annihilation path. (a) quenched *I-V* complex structure, (b) after two long bonds are broken, (c) saddle point configuration, (d) new bonds are about to form, and (e) perfect diamond crystalline structure is recovered.

contraction or expansion around a point defect caused by the relaxation of neighboring atoms due to restructuring of atomic bonds corresponding to the vacant atom site or extra atom added. The volume change due to this relaxation of neighboring atoms is called the *relaxation volume* V^{rel}. The overall effect of volume change, i.e., the *formation volume* $\Delta\Omega$, is $\Delta\Omega_V = V_V^{\mathrm{rel}} + \Omega$ for a vacancy and $\Delta\Omega_I = V_I^{\mathrm{rel}} - \Omega$ for an interstitial, where Ω is the volume per atom in crystalline silicon.

In our calculations, a single point defect is generated at the center of a crystal of 216 atoms at its equilibrium density with constant volume and periodic boundary conditions. The system is then fully relaxed in the same manner as described above for the calculations of the formation energy.[27] Since the simulation cell volume is fixed, introduction of a point defect and its subsequent relaxation induces an internal pressure in the system. For contraction (expansion) around a point defect, one expects a negative (positive) internal pressure. The reference state of a perfect crystal at its equilibrium density has zero pressure. By adjusting the volume of the defected system until zero pressure is recovered, one obtains the volume change after relaxation around a point defect. Thus, we obtain the relaxation volume of the point defect. A supercell of 216 atoms is found to be large enough since all atomic relaxation involved are found to be well confined within the simulation cell.

The internal pressure is calculated by $P = -\partial E/\partial V$, where the expression is derived analytically from the tight-binding total energy function. Since the volume change under pressure is determined by the compressibility of the system, we first calculate the bulk modulus B using the current model. At small volume changes, we obtain a linear curve relation between P-V, the slope of which gives us the bulk modulus $B = -\mathrm{V}\partial P/\partial V = 86.0 \pm 0.5$GPa. Compared to the experimental value of 97.8 GPa, the difference is about 10%. This close agreement gives us confidence that the volume-pressure behavior can be properly described by this model, which is a necessary condition to obtain reliable relaxation volumes.

Since the pressure of the defected system averages the

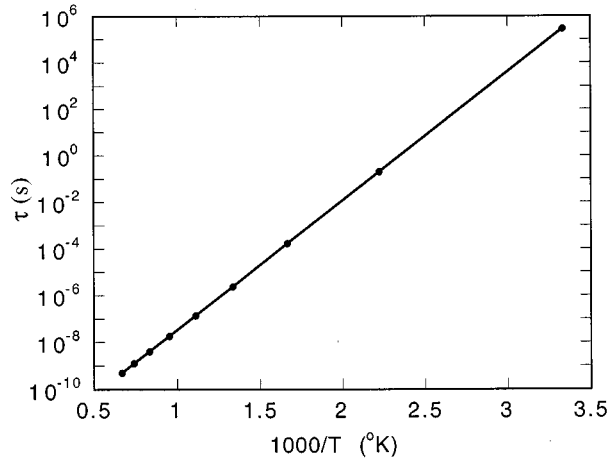

FIG. 9. Estimated I-V complex lifetime as a function of temperature.

effect of relaxation around a point defect over the whole simulation system, a small value of the internal pressure is expected for a single point defect. In order to obtain a reliable number for the volume change, an accurate comparison of pressure in the defected system and the perfect crystal is required. Using the lattice parameter value of 5.451 Å given in the original paper by Kwon *et al.*,[21] we obtain a pressure of -2.5×10^{-1} GPa for the undefected system. The pressures obtained with a vacancy and an interstitial are -7.4×10^{-1} and 1.1×10^{-1} GPa, respectively. These three pressures are all in the same order of magnitude, which suggests that the crystal is not in its perfect equilibrium state. Thus, we need to refine the lattice parameter to reach the true zero pressure reference state. We change the volume of the system by rescaling the length of our simulation box. Several iterations are performed until the pressure change of two consecutive trials and the absolute value of pressure itself are in the order of a convergence criterion of 10^{-4} GPa. If we define l/l_0 as the ratio between the current box length and the original box length corresponding to the lattice parameter of Kwon *et al.*, the new equilibrium box length is found to be $l_{\rm eq}/l_0=0.999\,042$ and the pressure is 2×10^{-4} GPa.

At $l_{\rm eq}$, the pressures for the fully relaxed vacancy and interstitial become -3.87×10^{-1} and 3.58×10^{-1} GPa, respectively. By rescaling the box lengths for the two defected systems until the pressures are within the same convergence criterion, we find the box length corresponding to the fully relaxed defect systems are $l_V/l_{\rm eq}=0.998\,508\,5$ and $l_I/l_{\rm eq}=1.001\,390\,3$ for the vacancy and interstitial, respectively. The relaxation volume in units of Ω, i.e., the atomic volume per silicon atom at the equilibrium density, is calculated by

$$V_{I,V}^{\rm rel}=\frac{l_{I,V}^3-l_{\rm eq}^3}{l_{\rm eq}^3/N}, \tag{9}$$

where $N=216$ in this study and $\Omega=l_{\rm eq}^3/N$. Thus, we obtain $V_V^{\rm rel}=-0.97\Omega$ and $V_I^{\rm rel}=0.90\Omega$ for vacancy and interstitial, respectively. The corresponding formation volumes are $\Delta\Omega_V=0.03\Omega$ and $\Delta\Omega_I=-0.10\Omega$.

Our calculated relaxation volumes are within 7% of each other in magnitude and have opposite sign. This result agrees well with recent diffuse x-ray scattering measurements.[20] In these measurements, Frenkel pairs are produced by electron irradiation at low temperature (4 K). The scattering amplitude and lattice constant change provide a measurement for the relaxation volumes by

$$S_H\propto c(V_V^{\rm rel^2}+V_I^{\rm rel^2}), \quad \text{and} \quad \Delta a/a\propto(V_V^{\rm rel}+V_I^{\rm rel}), \tag{10}$$

where S_H is the Huang scattering intensity. While an increase of S_H was observed at high electron dose, the lattice constant did not show any consistent increase. Therefore, it was concluded that the relaxation volumes of the vacancy and the interstitial must have opposite signs and cancel each other.[20] This conclusion, considering experimental error bars, is consistent with our calculations, where we obtained $V_V^{\rm rel}+V_I^{\rm rel}=-0.07\Omega$.

It is interesting to note that the vacancy formation volume in silicon was previously reported by Antonelli and Bernholc.[14] using pseudopotential LDA calculations. They obtained a relaxation volume of -0.25Ω or a formation volume of 0.75Ω, which is quite different from our results. The origin of these discrepancy likely lies in the fact that the LDA calculations of Antonelli and Bernholc were performed using a supercell of only 32 atoms. Recent studies show that in order to achieve good convergence, a supercell of 64 atoms with $2\times2\times2$ k-point mesh is necessary.[34] Second, in the LDA work of Antonelli and Bernholc, the relaxation volume was accounted for by only nearest-neighbor atom relaxations and no contribution was from the volume changes due to the relaxation of further shells of atoms. Because of the small size restriction, it is likely that only nearest-neighbor shell relaxation was significant in their calculation. But as found in our study using a large cell of 215 and 511 atoms for the fully relaxed vacancy structure, the displacements field can extend to the third and fourth nearest neighbors. The first shell displacement with respect to the equilibrium bond length is $\sim$20%; the second shell is $\sim$5–10 %; and the third and fourth shells are $\sim$1–5%. Therefore, both effects mentioned above in the LDA calculation of Antonelli and Bernholc would tend to underestimate the relaxation volume and give rise to a much larger formation volume for vacancy.

VI. DISCUSSION

As we have mentioned in Sec. III, despite decades of experimental work on self-diffusion in silicon, the only conclusive result is that $C_I^* d_I$ obeys Arrhenius behavior in the high-temperature range (1000–1300 °C) with an activation energy ranging from 4.7 eV to 5.1 eV and a prefactor ranging from 900 to 9000 cm^2/sec.[4] The activation energy and prefactor obtained from our calculations are 5.17 eV and 11555 cm^2/sec, respectively, which agrees well with the general picture. In addition, several experiments suggest a break of the Arrhenius behavior at about 1050 °C,[4] suggesting that different mechanisms operate above and below this temperature. Our calculations show that at 1080 °C, a crossover between I-dominated self-diffusion and V-dominated self-diffusion occurs.

Besides the product $C_I^* d_I$, however, little conclusive in-

formation exists regarding the individual terms C_I^* and d_I. This is because the value of d_I measured experimentally varies by almost ten orders of magnitude,[35] which is far beyond what could be expected from experimental uncertainties. The discrepancies concerning d_I were attributed to the much lower effective diffusivities of interstitials due to interactions with vacancies as proposed by Tan and Gösele.[36] In this so-called *vacancy-dominated effective I diffusivity* model, the resulting thermal equilibrium concentration of vacancies is much higher than interstitials while the vacancy diffuses much slower than the interstitial. Recently, the same authors have reinterpreted the much lower effective diffusivity of the interstitial based on trapping of interstitials by carbon atoms.[26] Gossmann *et al.*[37] have in fact shown that depending on C concentration in the matrix, the effective interstitial diffusivities can vary by many orders of magnitude. Stolk *et al.*[38] have shown that high C concentrations can be used to suppress TED which is mediated by excess interstitials from implantation damage. In this so-called *carbon-dominated effective I diffusivity* model, the resulting thermal equilibrium concentration of vacancies becomes much lower than that of interstitials and hence the vacancy diffusivity becomes higher than that of the interstitial, both of which are highly supported by our results shown in Fig. 1 and Fig. 4.

In addition to the magnitude of the interstitial diffusivity, our results also provide information on the atomistic mechanism of interstitial diffusion, as shown in Fig. 2. We have found that the neutral $\langle 110 \rangle$ dumbbell interstitial migrates via the tetrahedral site to a second nearest-neighbor lattice position where it again forms a $\langle 110 \rangle$ dumbbell. This is in contrast to interstitial diffusion in bcc and fcc metals, where $\langle 110 \rangle$ and $\langle 100 \rangle$ dumbbells migrate to a nearest-neighbor site by rotation and exchange of one of the two atoms with that site.[39] Recently, Nastar *et al.*[12] have investigated interstitial migration mechanisms in silicon using the Stillinger-Weber interatomic potential. In contrast to the results presented here, these authors found that there are actually two metastable dumbbell configurations and that the low-energy one is not actually the migrating species. They observed a two-stage migration mechanism consisting of a jump rotation followed by another rotation of the high-energy dumbbell. The source of the discrepancy between the tight-binding and the Stillinger-Weber results arises because the low-energy interstitial configuration obtained by the classical potential is actually a high-energy unstable or metastable configuration according to the tight-binding results. In fact, within the tight-binding calculations presented here, the high-energy dumbbell configuration (corresponding to the low-energy configuration with the classical potential) immediately relaxes to the low-energy configuration shown in Fig. 5 even at room temperature, so that it is either not a stable configuration within tight-binding, or the energy barrier is very small. Therefore, while a diffusion mechanism similar to that of Ref. 12 where the migrating species is a metastable defect is in principle possible, it is not feasible for the system studied within the tight binding model described here.

It has long been assumed that during interstitial injection due to surface oxidation steady state would be reached when[40]

$$C_I C_V = C_I^* C_V^* . \tag{11}$$

Thus during I injection, the vacancy undersaturation will be inverse proportional to interstitial supersaturation. However, the time to reach the steady state is determined by the interaction between interstitials and vacancies. If there is a barrier for the I-V annihilation process, the steady state will not be reached instantaneously. Our simulations of I-V interactions presented above are aimed to give a direct atomistic picture of I-V annihilation. We find that annihilation only occurs for very limited sites and that, instead, a complex defect is often formed as a result of the I-V interaction. Since the binding energy of the I-V complex with respect to separate I and V is very high (4.3 eV), its dissociation is very unlikely at all practical annealing temperatures. Therefore, the effect of formation of this I-V complex on the interstitial and vacancy concentration changes in the system seems to be no more different than the annihilation of the I-V pair. However, since the lifetime of the complex is estimated to be long at room-temperature, other effects are expected due to its existence. In particular, we expect the I-V complex to play an important role in the kinetics of silicon amorphization by light ions such as boron. It is well known that silicon cannot be amorphized by room temperature boron irradiation except at extremely high dose rates.[41] Since boron implantation gives rise to very diffuse damage distributions consisting mostly of isolated Frenkel pairs and small clusters,[42] we expect the stability of the I-V complex to play an important role in boron-induced silicon amorphization. For typical ion irradiation conditions, cascade overlap times are of the order of tenths of seconds to tens of seconds depending on dose rate. It is easy to see then how a I-V complex with an annihilation barrier of 1 eV could act as the rate-limiting factor in amorphization. If the dose rate is such that defects from one cascade can reach the debris from a previous one and annihilate the I-V complexes, then damage accumulation is too slow and no amorphization ensues. However, for high enough dose rates, damage accumulation can proceed very quickly without intracascade defect annihilation. We are presently following up and testing these ideas using a hybrid MD-kinetic Monte Carlo algorithm.

The long lifetime of the I-V complex at low temperatures suggests its existence in low-temperature electron irradiation experiments. As we discussed earlier, the experiments of Bausch *et al.*[20] showed that the total relaxation volume is zero for isolated Frenkel pairs. Will the existence of the I-V complex change the fact that the total relaxation volume is zero? To answer this question, we have also calculated the relaxation volume of the I-V complex as well as other possible close Frenkel pairs. We find that the relaxation volume of the I-V complex is 0.29Ω, which by itself will induce volume increase. However, possible close Frenkel pairs may contribute negative relaxation volumes. Our calculations confirm that the relaxation volumes for I-V pairs separated at third nearest-neighbor position along and perpendicular to the $\langle 110 \rangle$ dumbbell direction are -0.29Ω and -0.13Ω, respectively. Therefore, the total relaxation volume can still be very small with the coexistence of I-V complexes, separated Frenkel pairs and close Frenkel pairs.

VII. CONCLUSION

Within the tight-binding framework of Kwon *et al.*, we have revisited the fundamental aspects of intrinsic point de-

fects and diffusion in silicon. Our results show that the activation energy for vacancy diffusion is much lower than that for interstitial diffusion. The vacancy diffusivity was found to be higher than the interstitial diffusivity at all temperatures. For self-diffusion, however, our calculations, coupled with some experimental data and previous LDA results of the entropy of vacancy formation, clearly show that interstitials dominate self-diffusion at high temperature and vacancies dominate at low temperature. The crossover temperature is 1080 °C, which is in good agreement with the experimental estimate of 1050 °C.

The interaction of interstitials and vacancies can lead to formation of an *I-V* complex defect. This *I-V* complex has a very high binding energy of 4.3 eV, suggesting that it cannot dissociate at typical annealing temperatures. However, the annihilation barrier is of the order of 1 eV. This appears to indicate that the *I-V* complex could play an important role in the kinetics of room-temperature amorphization of silicon by light ion bombardment.

In addition, we have found that the relaxation volumes of interstitials and vacancies are close to each other in magnitude and opposite sign, which is in good agreement with experimental observations. The fact that both formation volumes are very small is in contrast to typical results in metals. For example, in fcc Au, the formation volumes are 0.56Ω and 0.44Ω for interstitials and vacancies, respectively. We believe this is due to the difference in the nature of atomic bonding and the resultant crystalline structures. In open structures such as that of silicon, small formation volumes are intuitively understandable. Similar results of formation volumes in germanium are expected.

ACKNOWLEDGMENTS

We acknowledge stimulating discussions with Dr. G. H. Gilmer, Dr. R. S. Averback, and Dr. P. B. Griffin. The work is performed under the auspices of the U.S. Department of Energy by Lawrence Livermore National Laboratory under Contract No. W-7405-Eng-48. We also wish to thank Dr. S. T. Dunham for useful discussions and providing access to the Boston University Center for Computational Science, where part of the calculations were performed. One of us (L.C.) acknowledges CILEA (Milano, Italy) for computational support under project ''Fisica Computazionale dei Materiali.'' We acknowledge partial financial support by NATO-Scientific Affairs Division under Contract No. CRG.950645.

[1] J. J. Wollenberger, in *Physical Metallurgy*, edited by R. W. Cahn and P. Haassen (North-Holland, New York, 1983), Pt. 2, p. 1139.

[2] E. Rimini, *Ion Implantation: Basics to Device Fabrication* (Kluwer Academic, Dordrecht, 1995).

[3] A. E. Michel, W. Rausch, P. A. Ronsheim, and R. H. Kastl, Appl. Phys. Lett. **50**, 416 (1987).

[4] P. M. Fahey, P. B. Griffin, and J. D. Plummer, Rev. Mod. Phys. **61**, 289 (1989).

[5] C. S. Nichols, C. G. Van de Walle, and S. T. Pantelides, Phys. Rev. Lett. **62**, 1049 (1989).

[6] P. E. Blochl, E. Smargiassi, R. Car, D. B. Laks, W. Andreoni, and S. T. Pantelides, Phys. Rev. Lett. **70**, 2435 (1993); R. Car, P. Blochl, and E. Smargassi, Mater. Sci. Forum **83-87**, 433 (1992).

[7] J. Zhu, L. H. Yang, C. Mailhiot, T. Diaz de la Rubia, and G. H. Gilmer, Nucl. Instrum. Methods B **102**, 29 (1995).

[8] Jing Zhu, T. Diaz de la Rubia, L. H. Yang, C. Mailhiot, and G. H. Gilmer, Phys. Rev. B **54**, 4741 (1996).

[9] G. H. Gilmer, T. Diaz de la Rubia, D. M. Stock, and M. Jaraiz, Nucl. Instrum. Methods Phys. Res. B **102**, 247 (1995).

[10] D. Maroudas and R. Brown, Phys. Rev. B **47**, 15 562 (1993).

[11] D. Maroudas and R. A. Brown, Appl. Phys. Lett. **62**, 172 (1993).

[12] M. Nastar, V. V. Bulatov, and Sidney Yip, Phys. Rev. B **53**, 13 521 (1996).

[13] U. Gösele and T. Y. Tan, in *Diffusion in Solids, Unsolved Problems* (Trans Tech Publications, Zurich, 1992), p. 189.

[14] A. Antonelli and J. Bernholc, Phys. Rev. B **40**, 10 643 (1989).

[15] H. R. Schober, Phys. Rev. B **39**, 13 013 (1989).

[16] Jing Zhu (unpublished).

[17] M. Ramamoorthy and S. T. Pantelides, Phys. Rev. Lett. **76**, 4753 (1996).

[18] H. Seong and L. J. Lewis, Phys. Rev. B **53**, 9791 (1996).

[19] C. Z. Wang and K. M. Ho, Comput. Mater. Sci. **2**, 93 (1994); L. Colombo, Annu. Rev. Comput. Phys. **4**, 147 (1996).

[20] St. Bausch, H. Zillgen, and P. Ehrhart (unpublished).

[21] I. Kwon, R. Biswas, C. Z. Wang, K. M. Ho, and C. M. Soukoulis, Phys. Rev. B **49**, 7242 (1994).

[22] L. Goodwin, A. J. Skinner, and D. G. Pettifor, Europhys. Lett. **9**, 701 (1989); C. Z. Wang, C. T. Chan, and K. M. Ho, Phys. Rev. Lett. **66**, 189 (1991).

[23] The *ab initio* results were obtained using a 64-atom supercell and with a $2\times2\times2$ *k*-point mesh. The results differ from Ref. 7 due to the use of the generalized gradient-corrected exchange and correlation functionals. Details of the calculation will be published elsewhere.

[24] H. Balamane, T. Halicioglu, and W. A. Tiller, Phys. Rev. B **46**, 2250 (1992).

[25] W. Frank, U. Gösele, H. Mehrer, and A. Seeger, in *Diffusion in Crystalline Solids*, edited by G. E. Murch and A. Nowick (Academic Press, New York, 1984), p. 31.

[26] U. Gösele, A. Plössl, and T. Y. Tan, in *Process Physics and Modeling in Semiconductor Technology*, edited by G. R. Srinivasan, C. S. Murthy, and S. T. Dunham (Electrochemical Society, Pennington, NJ, 1996), p. 309.

[27] M. Tang, L. Colombo, and T. Diaz de la Rubia, in *Ion-Solid Interactions for Materials Modification and Processing*, edited by D. B. Poker, Y.-S. Cheng, L. R. Harriott, and T. W. Sigmon, MRS Symposia Proceedings No. 396 (Materials Research Society, Pittsburgh, 1996), p. 33; L. Colombo, M. Tang, and T. Diaz de la Rubia, Phys. Scr. **T66**, 207 (1996).

[28] G. D. Watkins, in *Lattice Defects in Semiconductors, 1974*, Institute of Physics Conference Series No. 23, edited by F. A. Huntley (Institute of Physics, London, 1975), p. 1.

[29] G. D. Watkins, J. R. Troxell, and A. P. Chatterjee, in *Defects and Radiation Effects in Semiconductors, 1978*, Institute of Physics

Conference Series No. 46, edited by J. H. Albany (Institute of Physics, London, 1979), p. 16.
[30] S. A. Kahihara, D. J. Sullivan, Q. M. Zhang, T. A. White, and J. Bernholc (unpublished).
[31] M. D. Giles, J. Electrochem. Soc. **138**, 1160 (1991).
[32] D. A. Antoniadis and I. Moskowitz, J. Appl. Phys. **53**, 6788 (1982).
[33] U. Gösele, W. Frank, and A. Seeger, Solid. State Commun. **45**, 31 (1983).
[34] L. H. Yang, Jing Zhu, and J. S. Nelson (unpublished).
[35] W. Taylor, B. P. R. Marioton, T. Y. Tan, and U. Gösele, Radiat. Eff. Defects Solids **111**&**112**, 131 (1989).
[36] T. Y. Tan and U. Gösele, Appl. Phys. A **37**, 1 (1985).
[37] H.-J. Gossmann, P. A. Stolk, D. J. Eaglesham, G. H. Gilmer, and J. M. Poate, in *Process Physics and Modeling in Semiconductor Technology*, edited by G. R. Srinivasan, C. S. Murthy, and S. T. Dunham (Electrochemical Society, Pennington, NJ, 1996), p. 64.
[38] P. A. Stolk, D. J. Eaglesham, H.-J. Gossmann, and J. M. Poate, Appl. Phys. Lett. **66**, 1370 (1995).
[39] H. Dederichs, C. Lehmann, H. R. Schober, A. Schloz, and R. Zeller, J. Nucl. Mater. **69/70**, 176 (1978).
[40] E. Sirtl, in *Semiconductor Silicon* , edited by H. R. Huff and E. Sirtl (Electrochemical Society, Pennington, NJ, 1977), p. 4.
[41] R. Simonton, J. Shi, T. Boden, P. Maillot, and L. Larson, in *Materials Synthesis and Proceedings Using Ion Beams*, edited by R. J. Culbertson, O. W. Holland, K. S. Jones, and K. Maex, MRS Symposia Proceedings No. 316 (Materials Research Society, Pittsburgh, 1994), p. 153.
[42] M. J. Caturla, T. Diaz de la Rubia, L. Marques, and G. H. Gilmer, Phys. Rev. B **54**, 16 683 (1996).